

Synthesis, spectral characterization, SC-XRD, HSA, DFT and catalytic activity of a dioxidomolybdenum complex with aminosalicyl-hydrazone Schiff base ligand: An experimental and theoretical approach

Hadi Kargar^{a,*}, Mehdi Fallah-Mehrjardi^b, Reza Behjatmanesh-Ardakani^b,
Khurram Shahzad Munawar^{c,d}, Muhammad Ashfaq^{e,f}, Muhammad Nawaz Tahir^e

^a Department of Chemical Engineering, Faculty of Engineering, Ardakan University, P.O. Box 184, Ardakan, Iran

^b Department of Chemistry, Payame Noor University, 19395-3697 Tehran, Iran

^c Department of Chemistry, University of Sargodha, Punjab, Pakistan

^d Department of Chemistry, University of Mianwali, Mianwali, Pakistan

^e Department of Physics, University of Sargodha, Punjab, Pakistan

^f Department of Physics, University of Mianwali, Mianwali, Pakistan

ARTICLE INFO

Keywords:

Dioxidomolybdenum(VI) complex
Tridentate Schiff base
Selective oxidation
Solvent-free conditions
Homogeneous catalysis

ABSTRACT

A new dioxidomolybdenum(VI) complex has been successfully prepared by the reaction of an ONO donor Schiff base, derived by condensing 4-amino-2-hydroxybenzohydrazide and 3-methoxysalicylaldehyde, with MoO₂(a-cac)₂. The structures of synthesized products were explored spectroscopically through FT-IR, ¹H & ¹³C NMR and by elemental composition (CHN) through combustion analysis. The structural investigations of the dioxidomolybdenum(VI) complex were accomplished by taking its diffraction data through X-ray crystallography. The tridentate Schiff base ligand is bonded to the central metal through its deprotonated enolic and phenolic oxygen atoms and by the nitrogen of the azomethine group. The interpretation of the data obtained through diffraction analysis validates the distorted octahedral geometry of the prepared metal complex. QAIM, MEP and NCI calculations and Hirshfeld surface analysis were performed to investigate the nature and types of non-covalent linkages present among the sample molecules. The theoretical calculations, performed by DFT using the B3LYP/Def2-TZVP level of theory, direct that the intended outcomes are in compliance with the actual consequences. Furthermore, the catalytic potential of the molybdenum complex was explored for the selective oxidation of benzylic alcohols to the desirable aryl aldehydes at room temperature in the presence of 70% aqueous *tert*-butyl hydroperoxide (TBHP) under solvent-free conditions. The main advantage of the present catalytic work is the accomplishment of reaction in a short period of time, high percentage yield and easy work-out procedure.

1. Introduction

Schiff bases play an important part in the development and progress of the chemistry of chelated coordination compounds because of their significance in many interdisciplinary research fields [1–3]. Benzyl hydrazones, prepared by the condensation of hydrazides and aromatic aldehydes, are termed as vital Schiff base ligands because of their ability to alleviate the metals in several oxidation states along with diverse geometries [4,5].

In addition to this, aroylhydrazones got much more importance due to their structural flexibility, ease of preparation and steadiness against hydrolysis [6]. Another fascinating characteristic of aroylhydrazones is

that they exhibit either keto-enol tautomerism or E or Z configurational isomerism in solution form to modify themselves for different modes of coordination to form transition metal complexes [7,8]. Upon coordination with transition metal ions, the acidic protons are usually displaced and hence the aroylhydrazones behave in a dibasic fashion [9]. This deprotonation state of the ligand is responsible for the establishment of photophysical, electrochemical and catalytic properties [10].

The selective oxidation of primary alcohols into aldehydes is now becoming a topic of eminent curiosity due to the broad spectrum of their applications as intermediates in organic synthesis and in industries [11,12]. Nevertheless, it is a very difficult task to evade the over oxidation to carboxylic acids and to circumvent the use of harmful

* Corresponding author.

E-mail address: h.kargar@ardakan.ac.ir (H. Kargar).

<https://doi.org/10.1016/j.poly.2021.115428>

Received 31 May 2021; Accepted 12 August 2021

Available online 18 August 2021

0277-5387/© 2021 Elsevier Ltd. All rights reserved.

solvents. Many synthetic routes have been developed until now to accomplish the anticipated transformations by using the appropriate quantity of various oxidants [13]. The conventional methods adapted for the oxidation process involve the use of inorganic oxidants like chromates, chlorates permanganates, and oxides of various transition metals etc. [14,15]. Hence, a mixture consisting of organic substrates, solvents (usually chlorinated hydrocarbons), oxidants and products is very familiar with creating unavoidable explosions in several cases, as these protocols are performed under severe conditions of temperature and pressure [16].

Keeping in mind these restrictions, scientists are always excited about the development of environmentally friendly and harmless catalytic procedures for the oxidation of alcohols using some transition metal complexes together with O₂, H₂O₂, *tert*-BuOOH and, most preferably, solvent free routes [17]. Solvent free organic reactions have attained greater attraction due to several advantages, like high catalytic efficiency, selectivity, easy way of separation, non-tedious reaction conditions, simplicity and easy to work out [18–21].

The dioxidomolybdenum(VI) complexes have been successful in capturing the eyes of scholars due to their flexible approach towards reactivity, selectivity, and catalytic significance [22,23]. These dioxidomolybdenum(VI) complexes with aroylhydrazones have been studied extensively for various homogeneous and heterogeneous catalytic reactions, including selective oxidation of benzyl alcohols, epoxidation and sulfoxidation [24,25]. In these types of dioxo complexes, the ligand is usually doubly deprotonated and behaves in a tridentate fashion, and the sixth coordination site is usually occupied by the solvent molecule to form mononuclear complexes [23]. The attached solvent molecule is labile and facilitates the attachment of substrate molecules to complete the catalytic cycle [7].

Our research group has been engaged in the synthesis, characterization, catalytic potential and DFT studies of many of the Schiff base transition metal complexes in the last few years [26–30]. The present work is about the exploration of catalytic potential of the prepared dioxidomolybdenum(VI) complex for the conversion of benzyl alcohols to aryl aldehydes via *tert*-butyl hydroperoxide without the involvement of solvents.

2. Experimental

2.1. Materials and methods

Each and every chemical and solvent utilized in the current work is of reagent grade and procured from Acros Organics, Merck, and Sigma-Aldrich. The elemental composition (CHN) was determined by using Heraeus CHN-O-FLASH EA 1112 equipment. The multinuclear (¹H & ¹³C) NMR data was collected with the assistance of a BRUKER AVANCE 400 MHz spectrometer. The chemical shift values (δ) are assigned by comparing them with tetramethylsilane (TMS), an internal reference, whose value is arbitrarily fixed as zero ppm. The different functional groups present in the synthesized compounds were confirmed by running their infrared spectra after preparing potassium bromide pellets with the support of the IRPrestige-21 Spectrophotometer.

2.2. Preparation

2.2.1. Preparation of (*E*)-4-amino-2-hydroxy-*N'*-(2-hydroxy-3-methoxybenzylidene)benzohydrazide (H₂L)

H₂L was prepared by dissolving 4-amino-2-hydroxybenzohydrazide [31] (10 mmol, 1.67 g) and 3-methoxysalicylaldehyde (10 mmol, 1.52 g) separately in 50 mL of hot MeOH. The reactants were then mixed-up drop by drop and the resultant mixture was refluxed for approximately three hours until the reactants were completely converted into products as monitored by thin layer chromatography. For this, aliquots from the mixture were taken periodically to look for the disappearance of spots of reactants and the emergence of new spot of

product at a particular R_f value. After complete satisfaction with the accomplishment of the reaction, the contents were allowed to cool. Cooling of the reaction contents decreases the solubility and the product descends in the form of precipitates. The precipitates were then sorted out by the process of filtration under reduced pressure with the help of a rotary evaporator and cleansed in triplicate with cold methanol to purify them.

H₂L: Yield 67%. Anal. Calc. for C₁₅H₁₅N₃O₄: C, 59.80; H, 5.02; N, 13.95, Found: C, 59.91; H, 5.06; N, 14.07%. FT-IR (KBr, cm⁻¹): 3470 (ν_{N-H}); 1645 (ν_{C=O}); 1605 (ν_{C=N}); 1159 (ν_{C-O}); 1078 (ν_{N-N}). ¹H NMR (400 MHz, DMSO-*d*₆, ppm): 3.81 [3H, s, (H-C7)], 5.99 [2H, s, (—NH₂)], 6.03 [1H, (H-C12), d, ⁴J = 2.0 Hz], 6.14 [1H, (H-C14), dd, ³J = 8.8 Hz, ⁴J = 2.0 Hz], 6.86 [1H, (H-C4), t, ³J = 8.0 Hz], 7.02 [1H, (H-C3), dd, ³J = 8.0 Hz, ⁴J = 1.2 Hz], 7.12 [1H, (H-C5), dd, ³J = 8.0 Hz, ⁴J = 1.2 Hz], 7.63 [1H, (H-C15), d, ³J = 8.8 Hz], 8.60 [1H, s, (—CH=N)], 11.07 [1H, s, (—NH)], 11.76 [1H, s, (—OH)], 12.35 [1H, s, (—OH)]. ¹³C NMR (100 MHz, DMSO-*d*₆, ppm): 55.8 (C7) 99.3 (C12), 101.3 (C10), 105.9 (C14), 113.6 (C3), 118.9 (C6), 119.0 (C4), 120.8 (C5), 128.9 (C15), 147.0 (C2), 147.4 (C1), 147.9 (C8), 154.8 (C13), 162.8 (C11), 165.8 (C9).

2.2.2. Preparation of [Mo^{VI}O₂L(H₂O)] complex

The dioxidomolybdenum complex [Mo^{VI}O₂L(H₂O)] was prepared by suspending equimolar amounts of ligand H₂L (0.5 mmol, 0.150 g) along with MoO₂(acac)₂ (0.5 mmol, 0.165 g) in 50 mL of MeOH in a two necked flask with magnetic stirring over a hot plate. The stuffing of the suspension was refluxed for roughly three hours. After that, it was concentrated with the help of a rotary evaporator by creating an environment of reduced pressure to facilitate the evaporation of excess solvent. At the end, the flask was ice-cooled to procure the orange-coloured precipitates, which were then filtered and cleansed meticulously with diethyl ether and water, and then dehydrated in a desiccator under an inert atmosphere. A saturated solution of the prepared complex was made by dissolving it into a minimum volume of dimethyl formamide (DMF) to grow the crystals of the subject complex (MoO₂L(H₂O).2DMF) suitable for single crystal analysis.

[MoO₂L(H₂O)]: Yield 73%. Anal. Calc. for C₁₅H₁₅MoN₃O₇: C, 40.46; H, 3.40; N, 9.44, Found: C, 40.25; H, 3.34; N, 9.51%. FT-IR (KBr, cm⁻¹): 1597 (ν_{C=N}); 1456 (ν_{C=N-N-C}); 1253 (ν_{C-O}); 1055 (ν_{N-N}); 933 (ν_{O-Mo-O}) *asym*; 912 (ν_{O-Mo-O}) *sym*; 599 (ν_{Mo-O}); 451 (ν_{Mo-N}). ¹H NMR (400 MHz, DMSO-*d*₆, ppm): 3.81 [3H, s, (H-C7)], 6.04 [2H, s, (—NH₂)], 6.08 [1H, (H-C12), d, ⁴J = 2.0 Hz], 6.19 [1H, (H-C14), dd, ³J = 8.8 Hz, ⁴J = 2.0 Hz], 7.02 [1H, (H-C4), t, ³J = 8.0 Hz], 7.21 [1H, (H-C3), d, ³J = 8.0 Hz], 7.23 [1H, (H-C5), d, ³J = 8.0 Hz], 7.44 [1H, (H-C15), d, ³J = 8.8 Hz], 8.87 [1H, s, (—CH=N)], 11.32 [1H, s, (—OH)]. ¹³C NMR (100 MHz, DMSO-*d*₆, ppm): 55.8 (C7), 99.2 (C12), 100.7 (C10), 106.8 (C14), 116.4 (C3), 120.6 (C6), 121.6 (C4), 124.7 (C5), 130.4 (C15), 148.3 (C2), 148.6 (C1), 152.8 (C8), 154.8 (C13), 160.6 (C11), 169.7 (C9).

2.3. X-ray crystallographic data collection and structure determination of complex

The diffraction data of the dioxidomolybdenum(VI) complex (MoO₂L(H₂O).2DMF) was collected on the Bruker Kappa APEX-II CCD refractometer by employing molybdenum as a target material for the production of X-rays. A graphite-based monochromator is used for the generation of Mo-Kα radiation. The data was collected with the help of APEX-II software [32], while SADABS [33] software was employed for performing absorption corrections. The obtained raw data is resolved with the help of SHELXS-97 [34] software by using direct methods, while refinements of the data are executed by utilizing the full-matrix least-squares method on F₂ in SHELXL [35] software. Anisotropic displacement parameters were applied for the refinement of all atoms except hydrogen atoms. The placement of H-atoms at an ideal position was determined with the help of relative isotropic displacement parameters. For the graphical illustrations of the collected X-ray data of the

sample, ORTEP-3 [36], PLATON [37] and Mercury [38] software were used. The findings of the diffraction data of $\text{MoO}_2\text{L}(\text{H}_2\text{O})\cdot 2\text{DMF}$ is mentioned in Table S1.

2.4. Computational details

A Gaussian (09 version package) software [39] is used for density functional theory (DFT) calculations by employing the B3LYP level of theory [40] along with the Def2-TZVP basis set [41]. By considering the solvent, a solution phase was modelled by employing the IEFPCM [42]. Optimization of the geometry was verified by frequency analysis to make sure that all of the atoms are at their local minima on the molecular potential energy surface (PES). The absence of imaginary frequency was also revealed from the obtained results. The solution phase ^1H & ^{13}C NMR magnetic isotropic shielding tensors were calculated with the help of standard the Gauge-Independent Atomic Orbital (GIAO) method [43]. The chemical shifts (δ) of H_2L and its corresponding molybdenum complex were proposed with the help of the B3LYP method at the Def2-TZVP basis set and the IEFPCM model as an implicit model of the solvent and equated with the experimental findings in deuterated $\text{DMSO}-d_6$. All IEFPCM calculations for the prepared compounds were done by using the same solvent. The chemical shift values were computed by subtracting the suitable isotropic part of the shielding tensor from that of tetramethylsilane $\delta i = \sigma_{\text{TMS}} - \sigma_i$. The solution phase isotropic shielding constants for tetramethylsilane determined by B3LYP/Def2-TZVP level of theory were equal to 184.52 ppm for the ^{13}C and 31.92 ppm for the ^1H nuclei. The contour plots of the lowest unoccupied molecular orbital (LUMO) and the highest occupied molecular orbital (HOMO) were produced by using the Chemissian program [44]. Molecular electrostatic potential (MEP) data was deliberated with the Multiwfn program [45] and visualized with the help of VMD [46]. All types of non-covalent linkages were explored by the NCIPLOT [47] program. NBO calculations were also carried out by using the NBO 6.0 program [48].

2.5. Generalized method for the catalytic selective oxidation of benzylic alcohols by $\text{MoO}_2\text{L}(\text{H}_2\text{O})$ complex

The $\text{MoO}_2\text{L}(\text{H}_2\text{O})$ complex (0.6 mol%) was mixed to a 1 mmol solution of benzylic alcohol and a 2 mmol 70% aqueous solution of *tert*-BuOOH, and the contents of the reaction were continuously stirred at room temperature without the employment of solvent for a definite period of time. The catalytic conversion is continuously observed by employing thin layer chromatography by using a 70:30 mixture of *n*-hexane and diethyl ether as the eluent. On the accomplishment of the reaction, CH_3CN (10 mL) was added up and then the reacting stuff was filtered off to separate the catalyst in the form of residue. The residue was then washed thrice with cold CH_3CN (3×5 mL). The filtrate was concentrated under reduced pressure to get the respective benzaldehydes, which were then further refined with the help of column

chromatography by employing silica gel. The products gained after the completion of the catalytic cycle were characterized spectroscopically and then the data was compared with the standard samples.

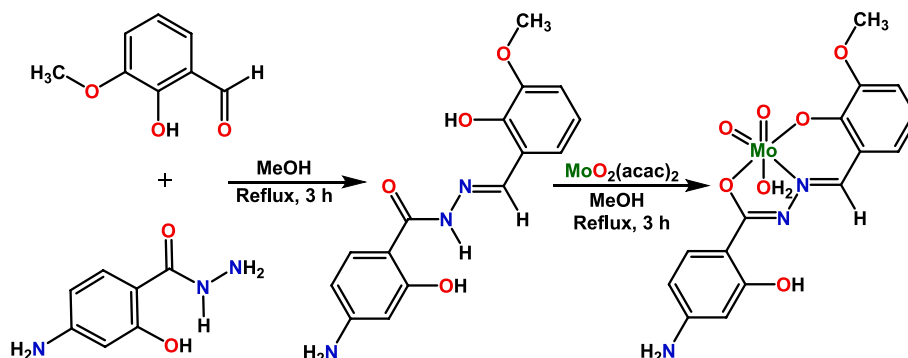
3. Results and discussion

3.1. Synthesis

An ONO-donor Schiff base ligand (H_2L) was synthesized by condensing equimolar amounts of 3-methoxysalicylaldehyde with 4-amino-2-hydroxybenzohydrazide in the presence of methanol as a solvent. Treatment of H_2L with $\text{MoO}_2(\text{acac})_2$ in refluxed MeOH gives out a targeted dioxidomolybdenum(VI) complex [$\text{MoO}_2\text{L}(\text{H}_2\text{O})$] (Scheme 1). The synthesized compounds were then characterized and finally, the catalytic potential of the $\text{MoO}_2\text{L}(\text{H}_2\text{O})$ was investigated for the selective oxidation of various substituted benzylic alcohols using aqueous TBHP as an oxidant.

3.2. Crystal structure analysis

In $\text{MoO}_2\text{L}(\text{H}_2\text{O})\cdot 2\text{DMF}$ (Fig. 1, Table S1), the asymmetric unit is composed of one molybdenum containing molecule (molecule I) and two non-coordinating dimethylformamide molecules (molecule II, C16-C18/N4/O8A), (molecule III, C19A-C21A/N5A/O9A). The coordination sphere of molybdenum ion was composed of O-atom of 2-methoxyphenolate moiety (O1), phenolic O-atom (O3), imine N-atom (N1) from the hydrazone part of the prepared ligand, O-atoms (O5/O6) of the dioxo groups, and one coordination site is occupied by O-atom of the coordinating water molecule as solvent (O7) which also acts as a ligand. The coordination of the tridentate chelating ligand with Mo-atom is established in such a way that the atoms of the whole hydrazone ligand are almost in the same plane. As a result of chelation, a six membered (Mo1/O1/N2/C1/C6/C8) and a five membered (Mo1/O3/N1/N2/C9) chelating rings are formed. In the coordination sphere, one of the oxo groups (O5) and the coordinating water molecule occupy axial sites, whereas (O1/O3/O6/N1) atoms occupy equatorial positions. The atoms of the equatorial plane are planar with a root mean square (r.m.s.) deviation of 0.0117 Å and the molybdenum atom is deviated by 0.3031 (2) Å from the equatorial plane towards the axial oxo group. In the coordination sphere, the bond lengths and bond angles (Table S2) are such that a distorted octahedral geometry is established in the titled compound. The anisole moiety A (C1-C7/O2) is oriented at dihedral angle of 6.67 (1)° with respect to 3-aminophenol group B. The intramolecular hydrogen bonding of type O—H...N stabilizes the molecular configuration of molybdenum containing molecules by forming a S (6) H-bonded loop as given in Table S3 and displayed in Fig. S1. The N—H...O bonding forms a R₂²(9) loop that interlinks the molecule I in the form of dimers as presented in Table S3. These dimers are further connected with each other by moderately weak C—H...O bonding. The combination of N—H...O and C—H...O bonding generates a R₄⁴(28) loop as



Scheme 1. Preparation of H_2L Schiff base ligand and its corresponding $\text{MoO}_2\text{L}(\text{H}_2\text{O})$ complex.

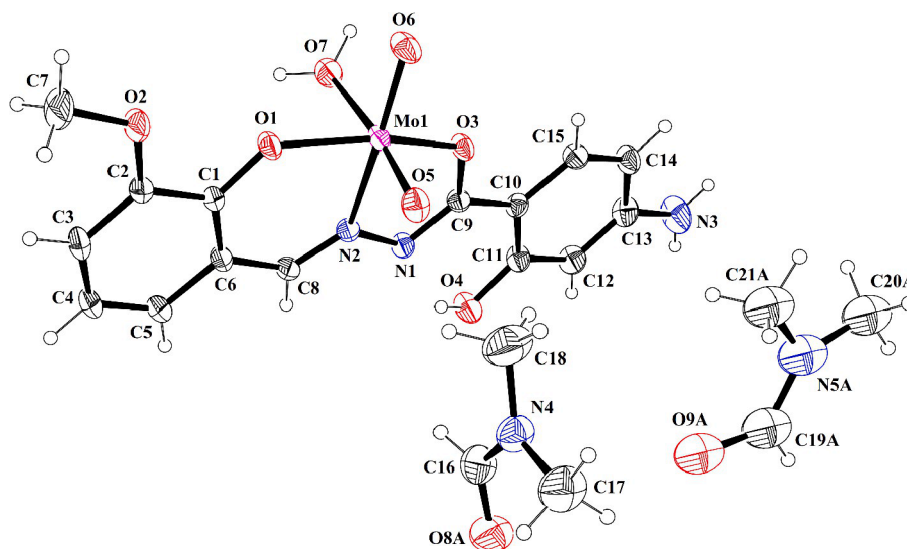


Fig. 1. Structural illustration of $\text{MoO}_2\text{L}(\text{H}_2\text{O})\cdot 2\text{DMF}$ drawn at a 50% probability level. Hydrogen atoms are shown in the form of small circles of arbitrary radii.

displayed in Fig. S2. A C20 zigzag chain is obtained by N3-H3A...O6 bonding that runs along the c-axis, whereas a C24 zigzag chain is obtained by the combination of N3-H3A...O6 and N3-H3B...O2 bonding. The H-bonding interactions interlink the molecules in such a way that an infinite one-dimensional chain of molecules is formed along the [101] crystallographic direction. Molecule II is connected with each other through C—H...O bonding. Likewise, molecule I and III are also interlinked through C—H...O bonding as given in Table S3. In addition to H-bonding, the crystal packing is further stabilized by off-set $\pi\cdots\pi$ stacking interaction with the inter-centroid varying from 3.56 to 4.39 Å (Fig. S3) and C—O... π interaction with H... π distance of 3.92 Å as given in Table S3 and shown in Fig. S4.

Investigation of non-covalent interactions is vital in building multi-dimensional structures and crystal engineering [49]. Single crystal data of $\text{MoO}_2\text{L}(\text{H}_2\text{O})$ indicated that the studied complex is self-assembled by intermolecular interactions. To analyze these non-covalent interactions, experimental coordination of two self-assembled $\text{MoO}_2\text{L}(\text{H}_2\text{O})$ units was employed for the calculations of molecular electrostatic potential (MEP), bond critical points (BCP), and non-covalent interaction index (NCI). QTAIM data showed that there are seven non-covalent interactions between two self-assembled $\text{MoO}_2\text{L}(\text{H}_2\text{O})$ units. Their electronic densities are in the range of 0.0011 a.u. (for $\pi\cdots\pi$ of $\text{Mo}=\text{O}\cdots\text{N}$) to 0.0080 a.u. (for $\text{CH}\cdots\text{O}$ hydrogen bond). Fig. S5 gives a detailed overview of the electronic densities of all non-covalent interactions. It is revealed from the graphical representation of self-assembled units that there are four kinds of hydrogen bonds and three kinds of $\pi\cdots\pi$ interactions between two units.

The calculated molecular electrostatic potential surface of the investigated dimeric unit $\text{MoO}_2\text{L}(\text{H}_2\text{O})$ is shown in Fig. S6. The calculated MEP values above the aromatic rings are in the range of -12 to -45 kcal.mol $^{-1}$. The results support the QTAIM data, which indicates that the aromatic rings are appropriate for $\pi\cdots\pi$ connections. Moreover, the non-covalent interaction index (NCI), which is a visualization tool based on density and its derivatives, is presented in Fig. S7. The Figure is shown by isosurfaces rather than critical points for better understanding of non-covalent interactions.

3.3. Geometrical parameters

The gas phase optimized geometrical parameters of the Schiff base ligand and its corresponding dioxidomolybdenum complex are shown in Fig. S11 and the optimized structural parameters, bond angles and bond lengths, for the $\text{MoO}_2\text{L}(\text{H}_2\text{O})$ complex obtained from DFT calculations,

B3LYP level of theory at the Def2-TZVP basis set, are given in Table S2 along with its X-ray diffraction data. It can be concluded from Table S2 that the computational particulates are fairly parallel with the actual experimental outcomes. The slight difference arises may be justified by the fact that experimental results were obtained from the sample in a solid state while the theoretical findings were based on considering the single molecule in an isolated gaseous form. Just like the diffraction data derived from X-ray analysis, the computational results also confirm the same distorted octahedral geometry around the molybdenum centre due to the coordination of oxygen and nitrogen atoms.

The Schiff base ligand H_2L deprotonates to L^{2-} and plays the role of a tridentate dianionic moiety in which one N and two O $^-$ atoms are coordinated to the central metal atom. The calculated N $_1$ —C $_8$ (1.290 Å) and N $_2$ —C $_9$ (1.315 Å) bond lengths are in close approximation to the HC=N double bond length (1.25 Å). The calculated C $_1$ —O $_1$ and C $_9$ —O $_3$ bond lengths are 1.333 and 1.316 Å, respectively, which are somewhat intermediate to the C=O (1.21 Å) and C—O bond lengths (1.43 Å). Also, the calculated bond lengths for C $_6$ —C $_8$, C $_1$ —C $_6$ and C $_9$ —C $_10$ are 1.440, 1.407 and 1.447 Å, respectively, which are smaller as compared to C—C single bond (1.54 Å) but larger than that of a C=C double bond (1.34 Å). It can be concluded from the values that electronic clouds may be delocalized over the azomethine moiety, carbonyl group, aromatic rings, and the C $_1$ —O $_1$ bond.

3.4. FT-IR and NMR study

Some particular theoretical and experimental FT-IR vibrational parameters of the synthesized ligand H_2L and its respective dioxidomolybdenum(VI) complex [$\text{MoO}_2\text{L}(\text{H}_2\text{O})$] are presented in Table 1. The percentage difference between both types of values is less than 6%, which is due to the implementation of the harmonic approximation for the calculations accomplished in the vacuum.

Experimental and theoretical FT-IR spectra of the ligand H_2L and its respective dioxidomolybdenum complex are presented in Figs. S12 and S13. As shown in Fig. S12, in the vibrational spectrum of the ligand, two very important peaks appear at 3470 and 1645 cm^{-1} are assigned to the stretching vibrational frequencies of the hydrazonic (NH) and carbonyl (C=O) groups. The absence of these particular aforesaid peaks in the spectrum of molybdenum complex is a clear-cut indication of deprotonation and involvement of these sites in coordination with metal [51]. Another sharp peak in the spectrum of H_2L due to the azomethine chromophore at 1605 cm^{-1} is switched to a lower wavenumber value (1597 cm^{-1}) during complex formation. This shifting is also attributed

Table 1The experimental and calculated infra-red vibrational parameters (cm^{-1}) along with relative errors of the H_2L ligand and $\text{MoO}_2\text{L}(\text{H}_2\text{O})$ complex.

Assignment	H_2L			$\text{MoO}_2\text{L}(\text{H}_2\text{O})$		
	Experimental	Calculated ^a	Relative error (%) ^b	Experimental	Calculated ^a	Relative error (%) ^b
$\nu_{\text{N-H}}$	3470	3387	-2.39	-	-	-
$\nu_{\text{C=O}}$	1645	1671	1.58	-	-	-
$\nu_{\text{C=N}}$	1605	1612	0.44	1597	1593	-0.25
$\nu_{\text{C-O}}$	1159	1174	1.29	1253	1250	-0.24
$\nu_{\text{Mo-O}}$	-	-	-	933	981	5.14
				912	948	3.95
$\nu_{\text{Mo-O}}$	-	-	-	599	590	-1.50
$\nu_{\text{Mo-N}}$	-	-	-	451	478	5.99

^a Scaling factor, 0.965 [50]^b Relative error (%) = $(X^{\text{Calc}} - X^{\text{Exp}}) * 100 / X^{\text{Exp}}$

to the involvement of this moiety in coordination [52]. Another indication of donor site contribution is the relocation of the absorption peak belonging to phenolic oxygen ($\nu_{\text{C-O}}$) in H_2L from 1159 to 1253 cm^{-1} upon complexation [53]. There is also a noticeable change in the stretching frequencies of NH_2 group in ligand from 3223 & 3373 cm^{-1} to 3167 & 3267 cm^{-1} upon the formation of a chelated metal complex. The *cis*- $\text{Mo}(\text{O})_2$ moiety shows its peculiar symmetric and asymmetric stretching vibrational peaks at 912 & 933 cm^{-1} , respectively. In addition to this, Mo-N and Mo-O peaks were observed at 451 & 599 cm^{-1} , respectively. These molybdenum associated peaks are in accordance with the closely analogous compounds hitherto documented in the literature [54].

The multinuclear (^1H & ^{13}C) NMR details of the synthesized ligand and its corresponding dioxidomolybdenum complex are given in the experimental part and the spectra are manifested in Figs. S14-S17. The two important peaks in the proton NMR spectrum of H_2L appear at $\delta = 12.35$ and 11.76 ppm are attributed to the phenolic protons, and a singlet detected at 11.07 ppm is due to the presence of the iminic proton ($-\text{NH}$). The peak of iminic proton and one of the phenolic protons faded away on coordination with metal. This is an indication that one of the phenolic oxygen atoms and a nitrogen atom are directly attached to the molybdenum after losing their protons. These changes imply that the enolic form of the ligand is coordinated with the MoO_2^{2+} core [55].

Furthermore, the signal for azomethine chromophore ($\text{HC}=\text{N}$) visible at $\delta = 8.60$ ppm in the spectrum of H_2L was deshielded and switched to a higher chemical shift value at $\delta = 8.87$ ppm upon complexation [56].

The ^{13}C NMR spectral studies of the complex $\text{MoO}_2\text{L}(\text{H}_2\text{O})$ revealed that the signals for $\text{C}=\text{O}$ (carbonyl), $\text{C}-\text{OH}$ (phenolic) and $-\text{CH}-$ (methine) are found at $\delta = 169.7$, 148.6 and 152.8 ppm, respectively. The carbon atoms present in close proximity of the complexing atoms (i. e., C9, C1 and C8) exhibited a significant swap in the location of their signals because of coordination, verifying the involvement of these species in complex formation. The remaining aromatic and aliphatic carbons of H_2L and $\text{MoO}_2\text{L}(\text{H}_2\text{O})$ are observed in their particular localities in accordance with the earlier reports [57]. The experimentally observed and computationally calculated NMR data of the prepared compounds are in close association with each other (Table S4).

3.5. Molecular orbitals analysis

The LUMO and HOMO energies of the frontier molecular orbitals and the difference in energy of these orbitals ($\Delta E = E_{\text{LUMO}} - E_{\text{HOMO}}$) for the prepared compounds (H_2L ligand & $\text{MoO}_2\text{L}(\text{H}_2\text{O})$ complex) were calculated by the B3LYP/Def2-TZVP method. As it is evident in Fig. 2, the ΔE for H_2L (*keto*), H_2L (*enol*) and $\text{MoO}_2\text{L}(\text{H}_2\text{O})$ are 3.928, 3.634 and 3.125 eV, correspondingly. It is obvious from the data that the ligand is

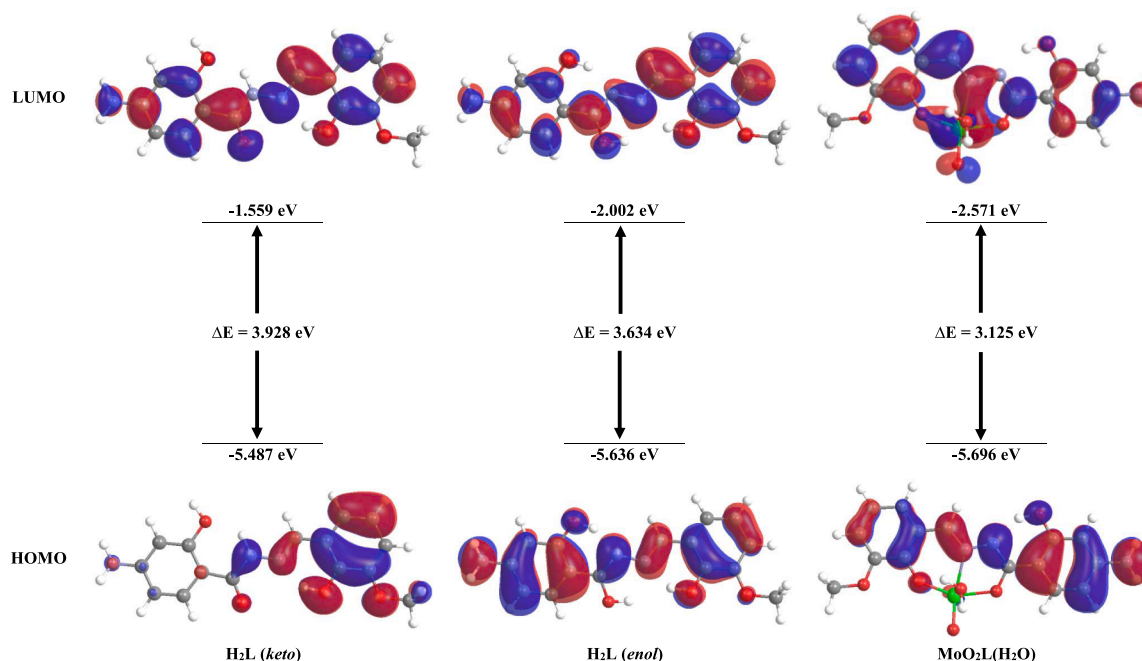


Fig. 2. Frontier molecular orbitals of the H_2L ligand (*keto* and *enol*) and $\text{MoO}_2\text{L}(\text{H}_2\text{O})$ complex.

more stable in keto form rather than in enol form due to higher ΔE value of 0.294 eV (6.8 kcal.mol⁻¹).

Therefore, the ligand in its enol form is softer than in its keto form and acts in a tridentate fashion upon interaction with molybdenum ion to produce the corresponding Mo(VI) complex. In the MoO₂L(H₂O) complex, the contributions of L and Mo to the molecular orbitals are: HOMO [100% L] and LUMO [35% L + 65% Mo]. It shows that Schiff base is a main contributor to HOMO, whereas the engagement of metal atom in this molecular orbital is insignificant. In contrast to this, Mo atom contributes significantly to LUMO due to the greater proclivity of metal to take electronic density.

3.6. Catalytic oxidation results

After successful synthesis and characterizing of MoO₂L(H₂O) complex, its catalytic efficiency was evaluated for the selective oxidation of benzylic alcohols. To sort out the reaction conditions, the oxidation of benzyl alcohol was selected as a model. In order to find a suitable solvent, different polar and non-polar solvents like methanol, ethanol, acetone, acetonitrile, chloroform, and dichloromethane were examined by using aqueous TBHP and catalytic quantity of MoO₂L(H₂O) complex. The results showed that the reaction did not complete in polar and non-polar solvents, although the use of less-polar solvents afforded a higher yield of the product. Interestingly, it was found that the best results were obtained under solvent-free conditions at room temperature (Table 2).

The effect of various oxidants like NaIO₄, H₂O₂, Bu₄NIO₄, UHP and TBHP was also tested in the oxidation of benzyl alcohol in the presence of MoO₂L(H₂O) catalyst under solvent-free conditions. It was revealed from the results that TBHP is considered as the best source of oxygen and it was also proved that the reaction did not perform well in the absence of the oxidant and only a small amount of the product was obtained. The investigation of the reaction in the presence of different amounts of oxidant showed that the conversion did not complete in the presence of less than 2 mmol of oxidant. The optimum amount of oxidant for the oxidation to aryl aldehyde was 2 mmol for the completion and production of benzaldehyde as the only product. The higher amount of oxidant had no discernible influence on the rate of the reaction and some benzoic acid was produced as a by-product (Table 3).

It is revealed from the data obtained that there would be no reaction in the absence of a catalyst. On increasing the amount of catalyst, the rate of reaction increases until the optimum value is achieved (0.6 mol %). A further increase in the quantity of the catalyst fails to produce any significant change in the yield (Table 4).

After obtaining the optimal reaction conditions, the selective oxidation of a wide range of benzylic alcohols carrying electron-donating and electron-withdrawing groups to their corresponding substituted benzaldehydes was evaluated under optimized conditions (Scheme 2, Table 5). It is obvious from Table 5 that all of the studied alcohols were completely converted into their respective aldehydes. The chemoselectivity of the procedure was remarkable. The benzyl alcohols were oxidized under the affection of this catalytic system and the desired

Table 2

The role of solvent for the oxidation of benzyl alcohol with TBHP in the presence of MoO₂L(H₂O).^a

Entry	Solvent	Yield (%) ^b	TON	TOF (h ⁻¹)
1	CH ₃ OH	48	80	40
2	CH ₃ CH ₂ OH	43	71.7	35.8
3	CH ₃ CN	29	48.3	24.2
4	CH ₃ COCH ₃	24	40	20
5	CHCl ₃	60	100	50
6	CCl ₄	69	115	57.5
7	Solvent-free	90	150	75

^a Reaction conditions: benzyl alcohol (1 mmol), TBHP (2 mmol), catalyst (0.6 mol%), solvent (5 mL), room temperature, 2 h

^b Isolated yield

Table 3

The effect of type and amount of oxidant on the oxidation of benzyl alcohol in the presence of MoO₂L(H₂O).^a

Entry	Oxidant	Oxidant amount (mmol)	Yield (%) ^b	TON	TOF (h ⁻¹)
1	No oxidant	0	10	16.7	8.3
2	NaIO ₄	2	30	50	25
3	UHP	2	67	111.7	55.8
4	H ₂ O ₂	2	56	93.3	46.7
5	TBHP	2	90	150	75
6	TBHP	1	46	76.7	38.3
7	TBHP	3	73	121.7	60.8

^a Reaction conditions: benzyl alcohol (1 mmol), oxidant, catalyst (0.6 mol%), room temperature, 2 h

^b Isolated yield

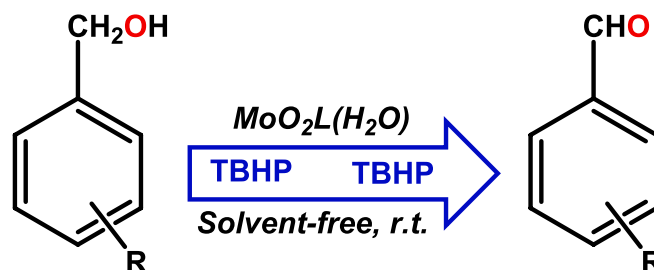
Table 4

Optimization of amount of catalyst for the oxidation of benzyl alcohol in the presence of MoO₂L(H₂O).^a

Entry	Catalyst amount (mmol)	Yield (%) ^b	TON	TOF (h ⁻¹)
1	0	15	–	–
2	0.002	34	170	85
3	0.004	65	162.5	81.2
4	0.006	90	150	75
5	0.008	92	115	57.5

^a Reaction conditions: benzyl alcohol (1 mmol), TBHP (2 mmol), catalyst, room temperature, 2 h

^b Isolated yield



Scheme 2. Selective oxidation of substituted benzyl alcohols catalysed by MoO₂L(H₂O).

Table 5

Selective oxidation of benzylic alcohols to benzaldehydes with TBHP catalysed by MoO₂L(H₂O) complex.^a

Entry	R	Time (min)	Yield (%) ^c	TON	TOF (h ⁻¹)
1	H	120	90	150	75
2	2-OMe	120	91	151.7	75.8
3	4-OMe	100	92	153.2	76.7
4	2-NO ₂	150	89	148.3	59.3
5	3-NO ₂	135	88	146.7	58.7
6	2-Br	120	92	153.2	76.7
7	4-Br	110	89	148.3	74.2
8	2-Cl	115	91	151.7	75.8
9	4-Cl	105	90	150	75
10	2,4-Cl ₂	180	91	151.7	50.6
11	4-OH	120	89	148.3	74.2

^aReaction conditions: benzylic alcohol (1 mmol), TBHP (2 mmol), catalyst (0.6 mol%), room temperature

^bAll products were identified by comparison of their physical and spectral data with those of authentic samples

^cIsolated yield

aryl aldehydes were obtained with 100% selectivity. It is interesting to note that in this procedure there was no overoxidation to benzoic acid derivatives took place with all the studied substrates. In addition, in the case of 4-hydroxybenzyl alcohol, the benzyl hydroxyl group is selectively oxidized while the phenolic hydroxyl group does not react at all (Entry 11).

It should be noted that the substituent position in the phenyl ring has certain steric effects on the reactivity of benzylic alcohols. For example, the substrate with a chloride substituent in the *ortho* position showed poor reactivity compared to the corresponding *para*-substitute benzyl alcohol (115 min. vs. 105 min.), and this fact could be due to the higher steric hindrance in the *ortho* position [58,59].

4. Conclusion

Current research work describes the synthesis of a tridentate (ONO) Schiff base ligand and its corresponding dioxidomolybdenum(VI) complex. The synthesized compounds were characterized by various spectroanalytical techniques. It was concluded from the results that the ligand behaves in a dianionic manner and exists in an enol form upon coordination. The molecular structure of the complex was determined by single crystal X-ray crystallography. The coordination geometry around Mo metal center was found to be distorted octahedral. Theoretical calculations of the Schiff base ligand and its Mo complex were carried out by DFT at the B3LYP/Def2-TZVP method. The results showed that theoretical data is in good consensus with the experimental outcomes. Furthermore, the catalytic activity of the complex has also been tested for the selective oxidation of benzylic alcohols to benzaldehydes by using aqueous TBHP under solvent-free conditions at room temperature. The developed protocol has many supremacies over the previously reported methods in terms of reduced reaction timings, simplicity, eco-friendly reaction conditions, higher yield and excellent selectivity to produce the corresponding aldehydes without any evidence of carboxylic acids formation.

5. Authors' statement

We would like to make an statement about the author's main contribution: HK synthesized all the compounds, and characterized them by different techniques; RBA and MFM designed the model and the computational framework and analysed the data; KSM, MA and MNT collected the single-crystal X-ray diffraction data and determined the structures. HK wrote the manuscript with input from all authors. All authors discussed the results and commented on the manuscript.

Declaration of Competing Interest

The authors declare that they have no known competing financial interests or personal relationships that could have appeared to influence the work reported in this paper.

Acknowledgments

We gratefully acknowledge the practical support for this study by Ardakan University and Payame Noor University.

Appendix A. Supplementary data

Supplementary data to this article can be found online at <https://doi.org/10.1016/j.poly.2021.115428>.

References

[1] B. Naureen, G.A. Miana, K. Shahid, M. Asghar, S. Tanveer, A. Sarwar, Iron (III) and zinc (II) monodentate Schiff base metal complexes: synthesis, characterisation and biological activities, *J. Mol. Struct.* 1231 (2021), 129946.

[2] A. Rauf, A. Shah, K.S. Munawar, A.A. Khan, R. Abbasi, M.A. Yameen, A.M. Khan, A. R. Khan, I.Z. Qureshi, H.-B. Kraatz, Zia-ur-Rehman, Synthesis, spectroscopic characterization, DFT optimization and biological activities of Schiff bases and their metal (II) complexes, *J. Mol. Struct.* 1145 (2017) 132–140.

[3] H. Kargar, A.A. Ardakani, K.S. Munawar, M. Ashfaq, M.N. Tahir, Nickel (II), copper (II) and zinc (II) complexes containing symmetrical tetradentate Schiff base ligand derived from 3, 5-diiodosalicylaldehyde: synthesis, characterization, crystal structure and antimicrobial activity, *J. Iran. Chem. Soc.* 18 (2021) 1–11.

[4] H. Kargar, M. Bazrafshan, M. Fallah-Mehrdar, R. Behjatmanesh-Ardakani, H. A. Rudbari, K.S. Munawar, M. Ashfaq, M.N. Tahir, Synthesis, characterization, crystal structures, Hirshfeld surface analysis, DFT computational studies and catalytic activity of novel oxovanadium and dioxomolybdenum complexes with ONO tridentate Schiff base ligand, *Polyhedron* 202 (2021), 115194.

[5] H. Kargar, P. Forootan, M. Fallah-Mehrdar, R. Behjatmanesh-Ardakani, H. A. Rudbari, K.S. Munawar, M. Ashfaq, M.N. Tahir, Novel oxovanadium and dioxomolybdenum complexes of tridentate ONO-donor Schiff base ligand: synthesis, characterization, crystal structures, Hirshfeld surface analysis, DFT computational studies and catalytic activity for the selective oxidation of benzylic alcohols, *Inorg. Chim. Acta* 523 (2021), 120414.

[6] S. Banerjee, A. Ray, S. Sen, S. Mitra, D.L. Hughes, R.J. Butcher, S.R. Batten, D. R. Turner, Pseudohalide-induced structural variations in hydrazone-based metal complexes: syntheses, electrochemical studies and structural aspects, *Inorg. Chim. Acta* 361 (2008) 2692–2700.

[7] V. Vrdoljak, B. Prugovečki, I. Pulić, M. Cigler, D. Sviben, J.P. Vuković, P. Novak, D. Matković-Čalogović, M. Cindrić, Dioxidomolybdenum (VI) complexes with isoniazid-related hydrazones: solution-based, mechanochemical and UV-light assisted deprotonation, *New J. Chem.* 39 (2015) 7322–7332.

[8] M. Sutradhar, T.R. Barman, A.J.L. Pombeiro, L.M.D.R.S. Martins, Aroylhydrazone Schiff base derived Cu(II) and V(V) complexes: efficient catalysts towards neat microwave-assisted oxidation of alcohols, *Int. J. Mol. Sci.* 21 (2020) 2832–2846.

[9] F. Chang, A. Kobayashi, K. Nakajima, H.-C. Chang, M. Kato, Dimensionality control of vapo-chromic hydrogen-bonded proton-transfer assemblies composed of a bis(hydrazone)iron(II) complex, *Inorg. Chem.* 50 (17) (2011) 8308–8317.

[10] S. Taktak, W. Ye, A.M. Herrera, E.V. Rybak-Akimova, Synthesis and catalytic properties in olefin epoxidation of novel iron(II) complexes with pyridine-containing macrocycles bearing an aminopropyl pendant arm, *Inorg. Chem.* 46 (7) (2007) 2929–2942.

[11] J.I. Kroschwitz, K. Othmer, *Encyclopedia of Chemical Technology*, Wiley-Interscience Publications, New York, NY, USA, 1992, pp. 64–72.

[12] F. Gaspar, C.D. Nunes, Selective catalytic oxidation of benzyl alcohol by MoO₂ nanoparticles, *Catalysts* 10 (2020) 265–279.

[13] S. Albonetti, R. Mazzoni, F. Cavani, Homogeneous, heterogeneous and nanocatalysis. In transition metal catalysis in aerobic alcohol oxidation; *Green Chemistry Series*; RSC: London, UK, (2014) 1–39.

[14] S.V. Ley, A. Madin, *Comprehensive Organic Synthesis*, Pergamon, Oxford, UK, 1991.

[15] M. Beller, The current status and future trends in oxidation chemistry, *Adv. Synth. Catal.* 346 (2004) 107–108.

[16] A.V. Biradar, M.K. Dongare, S.B. Umbarkar, Selective oxidation of aromatic primary alcohols to aldehydes using molybdenum acetylido oxo-peroxo complex as catalyst, *Tetrahedron Lett.* 50 (2009) 2885–2888.

[17] G. Veitch, A. Boyer, S. Ley, The azadirachtin story, *Angew. Chem., Int. Ed.* 47 (2008) 9402–9429.

[18] T. Kaicharla, S.R. Yetra, T. Roy, A.T. Biju, Engaging isatins in solvent-free, sterically congested Passerini reaction, *Green Chem.* 15 (2013) 1608–1614.

[19] L.-Y. Zhu, Z. Lou, J. Lin, W. Zheng, C. Zhang, J.-D. Lou, An efficient and selective oxidation of benzylic and aromatic allylic alcohols with manganese dioxide supported on kieselguhr under solvent-free conditions, *Res. Chem. Intermed.* 39 (2013) 4287–4292.

[20] J. Kamalraja, P.T. Perumal, Microwave assisted InCl₃ mediated regioselective synthesis of highly functionalized indolylpyran under solvent-free condition and its chemical transformation to indolyltriazolopyran hybrids, *Tetrahedron Lett.* 55 (2014) 3561–3564.

[21] M. Hatefi-Ardakani, S. Saeednia, Z. Pakdin-Parizi, M. Rafeezadeh, Efficient and selective oxidation of alcohols with tert-BuOOH catalyzed by a dioxomolybdenum (VI) Schiff base complex under organic solvent-free conditions, *Res. Chem. Intermed.* 42 (2016) 7223–7230.

[22] L. Balapoor, R. Bikas, M. Dargahi, Catalytic oxidation of benzyl-alcohol with H₂O₂ in the presence of a dioxidomolybdenum(VI) complex, *Inorg. Chim. Acta* 510 (2020), 119734.

[23] D. Cvijanović, J. Pisk, G. Pavlović, D. Šišak-Jung, D. Matković-Čalogović, M. Cindrić, D. Agustin, V. Vrdoljak, Discrete mononuclear and dinuclear compounds containing a MoO₂²⁺ core and 4-aminobenzhydrazone ligands: synthesis, structure and organic-solvent-free epoxidation activity, *New J. Chem.* 43 (2019) 1791–1802.

[24] M. Bagherzadeh, M. Amini, H. Parastar, M. Jalali-Heravi, A. Ellern, L.K. Woo, Synthesis, X-ray structure and oxidation catalysis of an oxido-peroxido molybdenum(VI) complex with a tridentate Schiff base ligand, *Inorg. Chem. Commun.* 20 (2012) 86–89.

[25] Y.D. Li, X.K. Fu, B.W. Gong, X.C. Zou, X.B. Tu, J.X. Chen, Synthesis of novel immobilized tridentate Schiff base dioxomolybdenum(VI) complexes as efficient and reusable catalysts for epoxidation of unfunctionalized olefins, *J. Mol. Catal. A: Chem.* 322 (2010) 55–62.

[26] K.S. Munawar, S. Ali, M.N. Tahir, N. Khalid, Q. Abbas, I.Z. Qureshi, S. Hussain, M. Ashfaq, Synthesis, spectroscopic characterization, X-ray crystal structure, antimicrobial, DNA-binding, alkaline phosphatase and insulin-mimetic studies of

- oxidovanadium(IV) complexes of azomethine precursors, *J. Coord. Chem.* 73 (16) (2020) 2275–2300.
- [27] H. Kargar, M. Fallah-Mehrjardi, R. Behjatmanesh-Ardakani, K.S. Munawar, M. Ashfaq, M.N. Tahir, Titanium(IV) complex containing ONO-tridentate Schiff base ligand: synthesis, crystal structure determination, Hirshfeld surface analysis, spectral characterization, theoretical and computational studies, *J. Mol. Struct.* 130653 (2021).
- [28] H. Kargar, R. Behjatmanesh-Ardakani, V. Torabi, M. Kashani, Z. Chavoshpour-Natanzi, Z. Kazemi, V. Mirkhani, A. Sahraei, M.N. Tahir, M. Ashfaq, K.S. Munawar, Synthesis, characterization, crystal structures, DFT, TD-DFT, molecular docking and DNA binding studies of novel copper(II) and zinc(II) complexes bearing halogenated bidentate N, O-donor Schiff base ligands, *Polyhedron* 23 (2020), 114988.
- [29] H. Kargar, R. Behjatmanesh-Ardakani, V. Torabi, A. Sarvian, Z. Kazemi, Z. Chavoshpour-Natanzi, V. Mirkhani, A. Sahraei, M.N. Tahir, M. Ashfaq, K. S. Munawar, Novel copper(II) and zinc(II) complexes of halogenated bidentate N, O-donor Schiff base ligands: synthesis, characterization, crystal structures, DNA binding, molecular docking, DFT and TD-DFT computational studies, *Inorg. Chim. Acta* 514 (2021), 120004.
- [30] H. Kargar, F. Aghaei-Meybodi, R. Behjatmanesh-Ardakani, M.R. Elahifard, V. Torabi, M. Fallah-Mehrjardi, M.N. Tahir, M. Ashfaq, K.S. Munawar, Synthesis, crystal structure, theoretical calculation, spectroscopic and antibacterial activity studies of copper(II) complexes bearing bidentate schiff base ligands derived from 4-aminoantipyrine: influence of substitutions on antibacterial activity, *J. Mol. Struct.* 1230 (2021), 129908.
- [31] H. Kargar, R. Kia, M.N. Tahir, 4-Amino-2-hydroxybenzohydrazide, *Acta Crystallogr. E*68 (2012), o2117.
- [32] Bruker, APEX2, Bruker AXS Inc., Madison, Wisconsin, USA, (2012).
- [33] G.M. Sheldrick, SADABS, Version 2.03. University of Göttingen, Germany, (2002).
- [34] G.M. Sheldrick, SHELXS97, SHELXL97, University of Göttingen, Germany, 1997.
- [35] G.M. Sheldrick, Crystal structure refinement with SHELXL, *Acta Crystallogr. C* 71 (2015) 3–8.
- [36] L.J. Farrugia, WinGX and ORTEP for Windows: An Update, *J. Appl. Crystallogr.* 45 (2012) 849–854.
- [37] A.L. Spek, Structure validation in chemical crystallography, *Acta Crystallogr. D* 65 (2009) 148–155.
- [38] C.F. Macrae, I. Sovago, S.J. Cottrell, P.T.A. Galek, P. McCabe, E. Pidcock, M. Platings, G.P. Shields, J.S. Stevens, M. Towler, P.A. Wood, Mercury 4.0: from visualization to analysis, design and prediction, *J. Appl. Crystallogr.* 53 (2020) 226–235.
- [39] M.J. Frisch, G.W. Trucks, H.B. Schlegel, G.E. Scuseria, M.A. Robb, J.R. Cheeseman, G. Scalmani, etc. GAUSSIAN 09 (Revision D.01), Gaussian, Inc., C. T. Wallingford, (2013).
- [40] A.D. Becke, Densityfunctional thermochemistry. III. The role of exact exchange, *J. Chem. Phys.* 98 (1993) 5648–5652.
- [41] J. Tomasi, B. Mennucci, R. Cammi, Quantum mechanical continuum solvation models, *Chem. Rev.* 105 (2005) 2999–3094.
- [42] F. Weigend, R. Ahlrichs, Balanced basis sets of split valence, triple zeta valence and quadruple zeta valence quality for H to Rn: design and assessment of accuracy, *Phys. Chem. Chem. Phys.* 7 (2005) 3297–3305.
- [43] J. Gauss, Effects of electron correlation in the calculation of nuclear magnetic resonance chemical shifts, *J. Chem. Phys.* 99 (1993) 3629–3643.
- [44] <http://www.chemissian.com>.
- [45] T. Lu, F. Chen, Multiwfn: a multifunctional wavefunction analyzer, *J. Comput. Chem.* 33 (2012) 580–592.
- [46] W. Humphrey, A. Dalke, K. Schulten, VMD: visual molecular dynamics, *J. Mol. Graph.* 14 (1996) 33–38.
- [47] E.R. Johnson, S. Keinan, P. Mori-Sánchez, J. Contreras-García, A.J. Cohen, W. Yang, Revealing noncovalent interactions, *J. Am. Chem. Soc.* 132 (2010) 6498–6506.
- [48] E.D. Glendening, J.K. Badenhoop, A.E. Reed, J.E. Carpenter, J.A. Bohmann, C. M. Morales, C.R. Landis, F. Weinhold, Theoretical Chemistry Institute, University of Wisconsin, Madison, WI, 2013.
- [49] D. Braga, F. Grepioni, Intermolecular interactions in nonorganic crystal engineering, *Acc. Chem. Res.* 33 (2000) 601–608.
- [50] M.A. Palafox, DFT computations on vibrational spectra: scaling procedures to improve the wavenumbers, *Phys. Sci. Rev.* 3 (2018) 1–30.
- [51] N. Majumder, S. Pasayat, S. Roy, S.P. Dash, S. Dhaka, M.R. Maurya, M. Reichelt, H. Reuter, K. Brzezinski, R. Dinda, Dioxidomolybdenum(VI) complexes bearing sterically constrained aroylazone ligands: synthesis, structural investigation and catalytic evaluation, *Inorg. Chim. Acta* 469 (2018) 366–378.
- [52] S. Pasayat, S.P. Dash, S. Roy, R. Dinda, S. Dhaka, M.R. Maurya, W. Kaminsky, Y. P. Patil, M. Nethaji, Synthesis, structural studies and catalytic activity of dioxidomolybdenum(VI) complexes with aroylhydrazones of naphthol-derivative, *Polyhedron* 67 (2014) 1–10.
- [53] X.-Q. He, Syntheses, X-ray structures, and catalytic oxidations of dioxomolybdenum(VI) complexes with tridentate benzohydrazones, *J. Coord. Chem.* 66 (2013) 966–976.
- [54] N.-Y. Jin, Syntheses, crystal structures, and catalytic properties of dioxomolybdenum(VI) complexes with hydrazone ligands, *J. Coord. Chem.* 65 (2012) 4013–4022.
- [55] R. Dinda, S. Ghosh, L.R. Falvello, M. Tomás, T.C.W. Mak, Synthesis, structure, and reactivity of some new dipyriddy and diamine-bridged dinuclear oxomolybdenum (VI) complexes, *Polyhedron* 25 (2006) 2375–2382.
- [56] T.M. Asha, M.R.P. Kurup, Synthesis, spectral characterization and crystal structures of dioxidomolybdenum(VI) complexes derived from nicotinoylhydrazones, *J. Chem. Crystallogr.* 49 (2019) 219–231.
- [57] N.K. Ngan, K.M. Lo, C.S.R. Wong, Synthesis, structure studies and electrochemistry of molybdenum(VI) Schiff base complexes in the presence of different donor solvent molecules, *Polyhedron* 30 (2011) 2922–2932.
- [58] R. Bikas, E. Shahmoradi, N. Noshiranzadeh, M. Emami, S. Reinoso, The effects of halogen substituents on the catalytic oxidation of benzylalcohols in the presence of dinuclear oxidovanadium(IV) complex, *Inorg. Chim. Acta* 466 (2017) 100–109.
- [59] R. Bikas, V. Lippolis, N. Noshiranzadeh, H. Farzaneh-Bonab, A.J. Blake, M. Siczek, H. Hosseini-Monfared, T. Lis, Electronic effects of aromatic rings on the catalytic activity of dioxidomolybdenum(VI)-hydrazone complexes, *Eur. J. Inorg. Chem.* 999–1006 (2017).